COMMUNICATION

Self-organized Gold Nanoreceptors on Silica nanoparticles for NMR Chemosensing

Federico De Biasi,†*[a] Daniele Rosa-Gastaldo,†*[a] Federico Rastrelli,*[a] and Fabrizio Mancin*[a]

[a] Dr. F. De Biasi, Dr. D. Rosa-Gastaldo, Prof. F. Rastrelli, Prof. F. Mancin
Department of Chemical Sciences
Università degli Studi di Padova
via Marzolo 1, 35131 Padova, Italy
E-mail: federico.debiasi@phd.unipd.it
daniele.rosagastaldo@unipd.it
federico.rastrelli@unipd.it
fabrizio.mancin@unipd.it

† F.D.B. and D.R.-G. contributed equally

Supporting information for this article is given via a link at the end of the document.

Abstract: "NMR-chemosensing" combines magnetization transfer NMR techniques with the recognition abilities of gold nanoparticles (AuNPs), allowing the direct and unambiguous detection of relevant organic species within complex mixtures without physical separation. In such experiments, sensitivity remains an issue, addressed so far only by enhancing the nanoreceptors' affinity for the analytes or the effectiveness of the NMR protocol. Here, we report a new strategy aimed at the improvement of the magnetization transfer efficiency, based on the enhancement of the nanoreceptors' size. With a fully non-synthetic approach, standard 2 nm AuNPs self-organized on the surface of commercially available 20 nm colloidal silica nanoparticles through electrostatic interactions. The so-formed supramolecular complexes allowed us to detect analytes in water down to 10 μM in 4 h using standard instrumentation.

Detection and identification of selected substances in complex mixtures are primary quests in many fields of chemistry, from environmental analysis to metabolomics, from drug detection to medical diagnosis. To this aim, the most commonly used procedures rely on chromatographic methods (HPLC, GC) which breaks down the complexity of the problem into the analysis of many fractions of fewer components.[1][other refs?] However, in these protocols, sample manipulation is time-consuming, and the possibility to perform direct analysis on the untreated sample is still highly desirable in order to optimize the experimental time and to minimize errors.

On such premises, Nuclear Magnetic Resonance (NMR) spectroscopy can be considered one of the most powerful techniques for the direct investigation of organic molecules. However, especially for proton-detected experiments, the wealth of information it delivers when applied straight on mixtures is often overwhelmed by spectral crowding. During the years, several advanced NMR techniques have been developed to (virtually) separate the mixtures' spectra in those of their single components. (*e.g.* diffusion-ordered spectroscopy, DOSY)[2,3] also taking advantage of external agents added to the sample with the purpose of selectively label certain signals. Namely, these latter experiments falls within the so-called molecule-assisted NMR techniques.[4–6] "NMR chemosensing" is one of them and exploits the recognition abilities of thiol-protected gold nanoparticles (AuNPs) to "extract" from that of the mixture the full ^{1}H-NMR spectrum of the species that bind to the coating monolayer.[5] This is usually achieved through the NOE-pumping experiment[7] or via Saturation Transfer Difference (STD) spectroscopy.[8] In both protocols, the magnetization transfer is governed by the Nuclear Overhauser Effect (NOE). Both approaches open the possibility to unambiguously identify the interacting analyte based on its spectral fingerprint, even in the puzzling case of an unknown sample composition. Yet, sensitivity remains a challenge: in the case of NOE-pumping the determined Limits Of Detection (LODs) rarely fall below the mM threshold even with hours-long experiments. Better performances (sub millimolar) were obtained with STD, but still with long acquisition times.[9,10] Recently, we demonstrated that this problem can be partially addressed (LOD of 50 μM in 1 h of acquisition) by innovative design of the NMR experiment. ~~Namely, a high-power water-mediated STD (HP wSTD) protocol was developed to exploit the water spins in long-lived association with the AuNPs monolayer as an additional reservoir of magnetization~~.[11]

In this communication, we report an innovative supramolecular evolution of the nanoreceptors that, with no synthetic effort, allowed us to break and further push down the remarkable LOD reached in the above example, optimizing with smart nanoreceptor design the magnetization transfer from the AuNPs to the interacting analytes

A more efficient magnetization transfer, resulting in stronger signals, can indeed be obtained by increasing the size of the nanoreceptors (see section 1 of ESI for a theoretical explanation). Nonetheless, the plain use of larger AuNPs in NMR chemosensing experiments may bring along several drawbacks. First, the enlargement of the core size requires a demanding fine-tuning of the synthetic procedures.[ref] Second, the characterization of the coating monolayer is not trivial in large AuNPs (extremely broad NMR signals, small thiol/gold ratio).[ref] Third, initial assessment of the recognition abilities of large AuNPs with NOE-pumping experiments (which are more reliable) is not possible because the enhanced transverse relaxation almost completely kills the AuNPs' magnetization during the spin echoes in the pulse sequence. Fourth, the analyte affinity for the nanoreceptor can be negatively affected by the decreased surface curvature.[12] last but not least, we also noticed that colloids comprising large (20 nm) charged nanoparticles are unstable when phosphate buffer is present in solution, even at low concentrations.

Our idea was that self-organized nanoconjugates obtained by the self-assembling of a corona of small AuNPs on the surface of large inert nanoparticles could provide the same benefits of large

nanoreceptors. Such nanoconjugates would be easier to synthesize compared to similarly sized AuNPs. Moreover, the nanoconjugates could form stable colloids in buffered samples. Several AuNPs previously used to detect designer drugs, biogenic amines and carboxylates, like **1**-AuNPs and **2**-AuNPs (Figure 1), are coated with charged monolayers. Hence, they could easily stick to the surface of bigger inorganic nanoparticles of opposite charge thanks to multiple ion-pairing interactions. As a consequence, the AuNPs' tumbling rate in solution would be sensibly lowered without remarkably affecting the local dynamics of the thiolate chains in the monolayer that is responsible for the binding affinity towards small analytes.[13] Commercially available colloidal amorphous silica nanoparticles (SiO_2NPs; LUDOX® HS, negatively charged, and LUDOX® CL, positively charged) appeared to best fit this scope as they are cheap and significantly larger (about 20 nm) than the typical 2 nm AuNPs used in chemosensing applications.

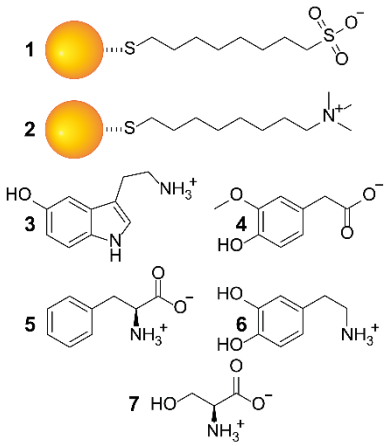

Figure 1. Gold nanoparticle and analytes used in this work: **1**: negatively charged AuNPs; **2**: positively charged AuNPs; **3**: serotonin; **4**: homovanillic acid; **5**: L-phenylalanine; **6**: dopamine; **7**: serine.

As a first step, we investigated the self-organization of the AuNPs@SiO_2NPs nanoconjugates. Diluted colloidal silica suspensions in phosphate saline buffer were analysed using Dynamic Light Scattering (DLS), obtaining an average particle size of 18 ± 1 nm, with a ζ-potential of 41.1 ± 0.7 mV for the LUDOX® CL, and −30.1 ± 0.8 mV for the LUDOX® HS. Upon the addition of oppositely charged AuNPs (section 2 of ESI), no significant variations in the particles size distributions were observed. On the other hand, the ζ-potentials shifted to neutral and eventually opposite values (− 22.5 ± 2.32 mV for **1**-AuNPs-LUDOX® CL and 34.1 ± 1.0 mV for **2**-AuNPs-LUDOX® HS). This suggested that the AuNPs were successfully assembling on the surface of the colloidal silica. Nevertheless, within a few minutes after their addition, we noticed the sedimentation of the nanoconjugates. This effect, likely due to the cross-linking ability of the AuNPs or to the overall charge neutralization of the AuNPs@SiO_2NPs aggregates, was prevented by adding polyethylene glycol (PEG) in the solution as surface-stabilizing agent. Besides its known ability to sterically stabilize silica colloids and the absence of charge (that should avoid interference in the analyte recognition process), PEG was chosen also because its ^{1}H-NMR spectrum in water only consists in a rather sharp singlet at 3.6 ppm, which does not interfere much in the NMR spectra. DLS experiments in the presence of PEG2000 confirmed the formation of nanoconjugates with similar size and ζ-potential, without any sedimentation for at least 5 h (largely exceeding the time needed for sample preparation and execution of the HP wSTD experiments).

We further confirmed the self-assembly of AuNPs on the surface of silica nanoparticles via TEM analysis. From the images reported in Figure 2 it appears how the gold nanoparticles (black dots) coated the surface of the silica nanoparticles (grey circles) forming a corona.

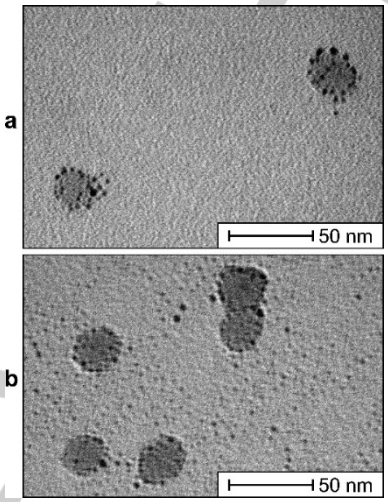

Figure 2. TEM micrography of the gold-silica supramolecular nanoconjugates. **a**: **1**-AuNPs on LUDOX® CL NPs. **b**: **2**-AuNPs on LUDOX® HS NPs. Gold nanoparticles appear as black spots while larger SiO_2NPs as grey circles.

Another evidence of the formation of the AuNPs@SiO_2NPs nanoconjugates, together with information about their composition (section 4 of ESI), was obtained by ^{1}H-NMR experiments. Small aliquots of a 1% w/w suspension of silica nanoparticles in a 0.01% w/w aqueous solution of PEG2000 were sequentially added to an NMR tube containing a solution of AuNPs 100 μM (in coating thiols) and phosphate buffer 200 μM in H_2O:D_2O=90:10. The ^{1}H-NMR spectra of the sample, recorded after every addition, showed a progressive disappearance of the signals of the coating monolayer due to the enhanced transverse relaxation and subsequent broadening of the resonances. This effect is caused by the lower tumbling rate of the AuNPs in solution as a result of their self-assembly on the surface of the SiO_2NPs. The titration of **2**-AuNPs with LUDOX® HS nanoparticles is reported in Figure 3 as an illustrative example.

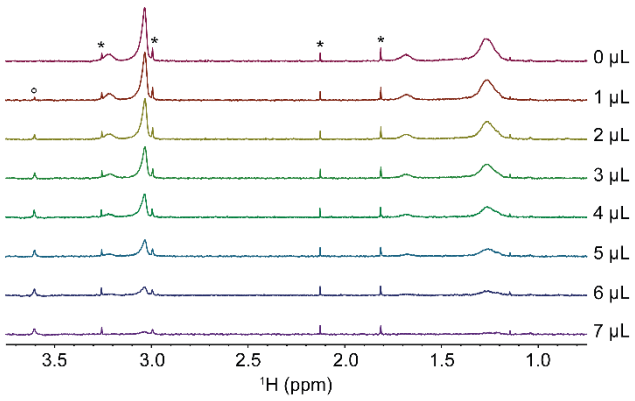

Figure 3. ^{1}H-NMR spectra of **2**-AuNPs 100 μM (in coating thiols) and phosphate buffer 200 μM in H_2O:D_2O=90:10 after subsequent additions of a suspension of LUDOX® HS silica nanoparticles (see the previous paragraph for details). Asterisks denote impurities while the circle indicates the PEG2000 signal.

In the NMR titrations, sedimentation was observed only after the addition of an excess of 1% w/w LUDOX® suspension, even in the presence of higher PEG2000 concentrations. This behaviour was different from that observed in the DLS experiments, where gold nanoparticles were present in slight excess after their addition and no sedimentation was observed. This suggests that stable nanoconjugates require, beside the presence of PEG, the formation of a complete AuNPs corona on the surface of the silica nanoparticles.

Having secured the formation of stable nanoconjugates, we moved to investigate their ability in the detection of selected analytes at low concentrations. **1**-AuNPs@LUDOX® CL were used to analyse a mixture of serotonin and phenylalanine 10 μM by means of HP wSTD experiments with a standard 500 MHz NMR spectrometer.[11] Results are reported in Figure 4, along with other HP wSTD spectra acquired in the absence of nanoparticles or including individually either AuNPs or SiO_2NPs. In agreement with theory and previous results, analyte signals were not detected in the absence of additives and in the presence of LUDOX® CL. More remarkably, also **1**-AuNPs alone were unable to produce signals above the LOD (set as signal intensity larger than three times the standard deviation of the noise). Only in the presence of the **1**-AuNPs@LUDOX® CL aggregates (panel **e** of Figure 4), all serotonin signals appeared in the processed STD spectrum. Nicely enough, signals of phenylalanine, which has no affinity for **1**-AuNPs, were not detected in any spectrum, confirming that the nanoreceptor abilities of **1**-AuNPs are not sensibly altered by their adsorption on colloidal silica for what concerns our experiments.

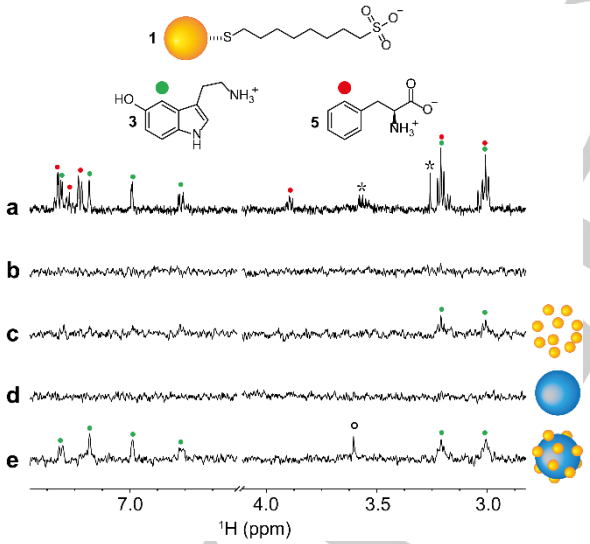

Figure 4. a: ^{1}H-NMR spectrum of serotonin (**3**) 10 μM and L-phenylalanine (**5**) 10 μM in H_2O:D_2O=90:10 in the presence of phosphate buffer 200 μM (pH=7); **b**-**e**: HP wSTD spectra performed on the sample presented in **a** in the absence of nanoparticles (**b**), in the presence of **1**-AuNPs (**c**), in the presence of LUDOX® CL nanoparticles (**d**) and in the presence of the nanoconjugates (**e**). Only in the latter case, all serotonin signals were detected. Asterisks denote impurities while the circle indicates the resonance of PEG2000 used to stabilize the aggregates. Whether present, **1**-AuNPs concentration was 20 μM in coating thiols. No of scans?

The same set of experiments was repeated using the system with opposite charges. **2**-AuNPs@LUDOX® HS were used to detect 10 μM homovanillic acid, a typical catecholamine metabolite, again in the presence of phenylalanine as model of possible interfering species.[14,15] Results are shown in Figure 5. In this case, two artefact singlets stemming from homovanillic acid do appear also in the control spectrum with no additives (panel **b** of Figure 5). Indeed, these singlets resonate too close to the water signal and receive excess irradiation from the HP saturating field required by the wSTD experiment.[11,16] Nonetheless, all the homovanillic acid resonances were detected only in the presence of the supramolecular nanoconjugates. Again, selectivity over non-recognized analytes was confirmed by the absence of phenylalanine signals in Figure 5**e**. Figure 5 also puts in evidence an additional advantage of the approach proposed here, which is the complete suppression of residual nanoparticles signals in the HP wSTD spectra due to their enhanced transverse relaxation. This avoids any possible interference generated from the overlap between the signals of the nanoparticles and those of the analytes.

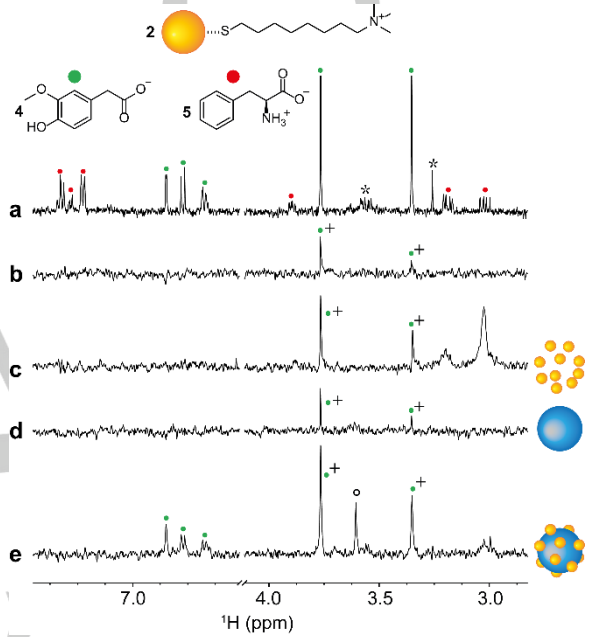

Figure 5. a ^{1}H-NMR spectrum of homovanillic acid (**4**) 10 μM and L-phenylalanine (**5**) 10 μM in H_2O:D_2O=90:10 in the presence of phosphate buffer 200 μM (pH = 7). **b**-**e** HP wSTD spectra performed on the sample presented in **a** in the absence of nanoparticles (**b**), in the presence of **2**-AuNPs (**c**), in the presence of LUDOX® HS nanoparticles (**d**) and in the presence of the nanoconjugates (**e**). Only in the latter case, all homovanillic acid signals were detected. A plus symbol is used here to indicate overly enhanced resonances. Asterisks denote impurities while the circle indicates the resonance of PEG2000 used to stabilize the aggregates. Whether present, **2**-AuNPs concentration was 20 μM in coating thiols. The broad signals in **c** at around 3.1 ppm stem from the monolayer of **2**-AuNPs. No of scans?

Comforted by the retained selectivity of the nanoreceptors upon their interaction with silica nanoparticles, as well as by the observed improved sensitivity, we repeated the HP wSTD experiments on mixtures containing more than two analytes where the binding candidates were present at 10 μM concentration while other three interferents were present at 20 μM concentration. Both mixtures were composed by dopamine (**6**, binding candidate for the **1**-AuNPs-LUDOX® CL nanoconjugates), homovanillic acid (**4**, binding candidate for the **2**-AuNPs-LUDOX® HS nanoconjugates), L-phenylalanine (**5**) and serine (**7**). Results are presented in Figure 6, where only the aromatic portion of the spectra is reported. From the traces, it is evident that both types of nanoconjugates continued to retain their selectivity towards their respective binding candidates also in the presence of more than one interferent, even when the latter were present at a higher concentration than that of the binding candidate. Notably, the

sensitivity improvement showed by the nanoconjugates was still rather remarkable.

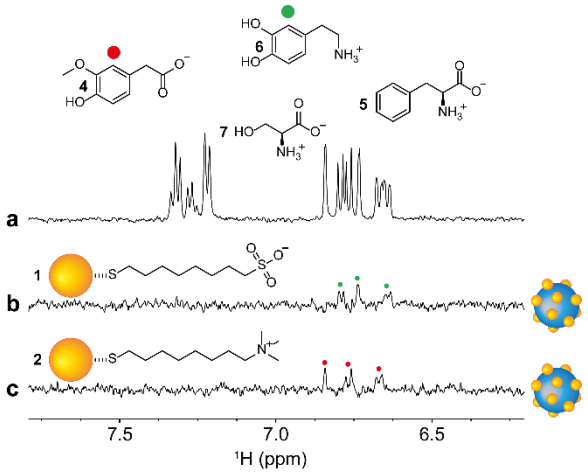

Figure 5. a: ^{1}H-NMR spectrum of a mixture of dopamine (**6**), homovanillic acid (**4**), L-phenylalanine (**5**) and serine (**7**) all 20 µM in H_2O:D_2O=90:10 in the presence of phosphate buffer 500 µM (pH=7); **b**-**c**: HP wSTD spectra performed on samples similar to that presented in **a** but in which the concentration of only the binding candidate was lowered down to 10 µM (dopamine for **b** and homovanillic acid for **c**). Both HP wSTD experiments were executed in the presence of the nanoconjugates (**1**-AuNPs-LUDOX® CL nanoconjugates for **b** and **2**-AuNPs-LUDOX® HS nanoconjugates for **c**). In both HP wSTD experiments the AuNPs concentration was 20 µM in coating thiols.

In conclusion, we have demonstrated that self-organized nanoconjugates prepared by assembling small AuNPs on the surface of LUDOX® silica nanoparticles allowed to obtain nanoreceptors that maintained the recognition properties of small monolayer protected nanoparticles while acquiring a more efficient magnetization transfer ability thanks to the lowered tumbling rate. This approach allowed to further decrease the LOD of nanoparticle-assisted NMR chemosensing to 10 µM, enabling its application to direct analysis of relevant targets. Note, as an example, that homovanillic acid concentration in children's urine above 10 µM can be related to the occurrence of the neuroblastoma tumour.[ref] In addition, the modularity of the presented method may allow the easy modification and tuning of the sensing systems.

Acknowledgements

Acknowledgements Text.

Keywords: keyword 1 • keyword 2 • keyword 3 • keyword 4 • keyword 5

[1] W. M. . Niessen, A. . Tinke, *J. Chromatogr. A* **1995**, *703*, 37–57.

[2] C. S. Johnson, *Prog. Nucl. Magn. Reson. Spectrosc.* **1999**, *34*, 203–256.

[3] M. Nilsson, G. A. Morris, *Chem. Commun.* **2007**, 933.

[4] J. Reuben, *Prog. Nucl. Magn. Reson. Spectrosc.* **1973**, *9*, 3–70.

[5] B. Perrone, S. Springhetti, F. Ramadori, F. Rastrelli, F. Mancin, *J. Am. Chem. Soc.* **2013**, *135*, 11768–11771.

[6] N. K. J. Hermkens, N. Eshuis, B. J. A. Van Weerdenburg, M. C. Feiters, F. P. J. T. Rutjes, S. S. Wijmenga, M. Tessari, *Anal. Chem.* **2016**, *88*, 3406–3412.

[7] A. Chen, M. J. Shapiro, *J. Am. Chem. Soc.* **2000**, *122*, 414–415.

[8] M. Mayer, B. Meyer, *Angew. Chemie Int. Ed.* **1999**, *38*, 1784–1788.

[9] M.-V. Salvia, F. Ramadori, S. Springhetti, M. Diez-Castellnou, B. Perrone, F. Rastrelli, F. Mancin, *J. Am. Chem. Soc.* **2015**, *137*, 886–892.

[10] L. Gabrielli, D. Rosa-Gastaldo, M.-V. Salvia, S. Springhetti, F. Rastrelli, F. Mancin, *Chem. Sci.* **2018**, *9*, 4777–4784.

[11] F. De Biasi, D. Rosa-Gastaldo, X. Sun, F. Mancin, F. Rastrelli, *J. Am. Chem. Soc.* **2019**, *141*, 4870–4877.

[12] M. Lucarini, P. Franchi, G. F. Pedulli, C. Gentilini, S. Polizzi, P. Pengo, P. Scrimin, L. Pasquato, *J. Am. Chem. Soc.* **2005**, *127*, 16384–16385.

[13] L. Riccardi, L. Gabrielli, X. Sun, F. De Biasi, F. Rastrelli, F. Mancin, M. De Vivo, *Chem* **2017**, *3*, 92–109.

[14] S. Barco, I. Gennai, G. Reggiardo, B. Galleni, L. Barbagallo, A. Maffia, E. Viscardi, F. De Leonardis, V. Cecinati, S. Sorrentino, et al., *Clin. Biochem.* **2014**, *47*, 848–852.

[15] V. Strenger, R. Kerbl, H. J. Dornbusch, R. Ladenstein, P. F. Ambros, I. M. Ambros, C. Urban, *Pediatr. Blood Cancer* **2007**, *48*, 504–509.

[16] B. Cutting, S. V. Shelke, Z. Dragic, B. Wagner, H. Gathje, S. Keim, B. Ernst, *Magn. Reson. Chem.* **2007**, *45*, 720–724.

[17] D. Neuhaus, M. P. Williamson, *The Nuclear Overhauser Effect in Structural and Conformational Analysis*, Wiley-VCH, **2000**.

Entry for the Table of Contents

Insert graphic for Table of Contents here.

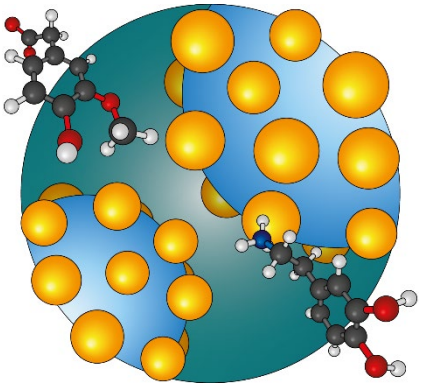

Insert text for Table of Contents here. ((The Table of Contents text should give readers a short preview of the main theme of the research and results included in the paper to attract their attention into reading the paper in full. The Table of Contents text **should be different from the abstract** and should be no more than 450 characters including spaces.))

Institute and/or researcher Twitter usernames: ((optional))